Wood cellulose films regenerated from NaOH/urea aqueous solution and treated by hot pressing for food packaging application

Kehao Huang[1], Anne Maltais[2], Jinxia Liu[3], Yixiang Wang[1*]

[1]Department of Food Science and Agricultural Chemistry, McGill University, Ste Anne de Bellevue, Quebec, H9X 3V9, Canada

[2]Institut de Technologie des Emballages et du Génie Alimentaire (ITEGA), Montréal, Québec, H1N 1C1, Canada

[3]Department of Civil Engineering, McGill University, Montreal, Quebec, H3A 0C3, Canada

Kehao Huang, kehao.huang@mail.mcgill.ca

Anne Maltais, amaltais@cmaisonneuve.qc.ca

Jinxia Liu, jinxia.liu@mcgill.ca

*Corresponding author: yixiang.wang@mcgill.ca

Abstract

Cellulose films made from 'green' solvent provide the possibility to mitigate environmental pollution caused by non-degradable plastic packaging. Herein, regenerated cellulose films were prepared from five wood pulps in NaOH/urea aqueous solution, dried either at ambient conditions or by hot pressing, and tested as biodegradable packaging materials. The results revealed that different wood origins did not cause much difference in the structure of cellulose films. However, hot-pressing could not only efficiently remove water from wet films, but also significantly improve the tensile strength and water vapor barrier property of regenerated films. The RC-P-HP film had the tensile strength of 85.00±3.26 MPa, Young's modulus of 6.45±0.36 GPa, and water vapor permeability of $3.59\pm0.14\times10^{-7}$ $gm^{-1}h^{-1}Pa^{-1}$, and exhibited the similar capacity as the commercial plastic wrap during the preservation of cherry tomatoes for up to 16 days. Therefore, this study demonstrates a feasible strategy to fabricate wood cellulose films for biodegradable food packaging.

Keywords: Wood pulps; cellulose films; regeneration; hot pressing; food packaging

1. Introduction

Food packaging waste accounts for approximately one-third of all household waste in Canada (Diggle & Walker, 2020). Among them, plastic waste has low secondary market value and high resistance to degradation and only 20% is collected for reuse and recycling (Diggle et al., 2020; Huang & Wang, 2022). The accumulation of this non-degradable waste has severe impacts on marine and terrestrial ecosystems, resulting in the urgent demand for eco-friendly food packaging materials. Cellulose is the most abundant biopolymer and has been explored as a potential alternative to petroleum-based plastics owing to its availability, renewability, and biodegradability (Shi et al., 2022). Wood is the most important source of cellulose, and the type of wood (e.g. hardwood and softwood) and processing conditions such as pulping and bleaching can affect the structure of isolated cellulose (Tang et al., 2021). Wood cellulose has been studied for applications in papermaking, textiles, biomedical, and high-performance materials (Jia et al., 2018). Recently, the development of packaging materials from wood cellulose nanofibrils (CNF) has been reported. For example, Missio et al. (2020) fabricated an antioxidative film by combining CNF from *Acacia mearnsii* bark and tannins. Tayeb et al. (2020) developed an oil barrier packaging material using CNF from a bleached softwood kraft pulp, and Muthoka et al. (2021) infiltrated CNF and chitosan into bleached fir veneer wood to form a transparent package.

Besides the utilization of CNF, natural cellulose fibers can also be easily converted into different materials through dissolution and regeneration (Huang, Wang, Zhang, & Chen, 2016). Traditional solvents for cellulose dissolution, such as *N*-methylmorpholine-*N*-oxide (NMMO), LiCl/DMAc, and ionic liquids (ILs), have significant disadvantages involving tedious handling processes, high energy consumption, and/or inefficient recyclability (Huang et al., 2016). The NaOH/urea aqueous system is a “green” solvent of cellulose that can disrupt the intra-/intermolecular hydrogen bonds of the supramolecular structure within cellulose (Cai & Zhang, 2005). It has been reported that the NaOH/urea system can be used to rapidly dissolve unbleached softwood kraft

pulp and spruce pulp at low temperatures after a mechanical or chemical pretreatment (Shi et al., 2018). However, the structure and properties of regenerated cellulose (RC) films from various wood pulps have not yet been well studied. Moreover, drying methods of cellulose films, such as air drying, freeze-drying, oven drying, and hot pressing, can also affect the performance of the films. Among them, hot pressing is a convenient way to dry cellulose films in a short time using elevated temperatures and pressures (Rol et al., 2020). Qing et al. (2015) found that the hot-pressed cellulose nanofibril (CNF) films showed improved mechanical properties compared to the freeze-dried and air/oven-dried samples. Similar results were observed by Hasan et al. (2021) that the CNF films treated by hot pressing exhibited decreased water vapor and oxygen permeability due to better consolidation of layers in the film structures.

Therefore, to develop wood cellulose films as biodegradable food packaging materials, in this work, various hardwood (aspen, eucalyptus, and maple) and softwood (pine and spruce) pulps were dissolved in NaOH/urea aqueous solution, and the corresponding RC films were dried either in the air at 25 °C or by hot pressing. The structure and properties of RC films were characterized, and the RC film with the best mechanical and barrier properties was selected to preserve fresh cherry tomatoes.

2. Materials and methods

2.1. Materials

The bleached kraft pulps of aspen, eucalyptus, maple, pine, and spruce were kindly provided by FPInnovations (QC, Canada). Sulfuric acid (95.0%-98.0%) was purchased from Sigma-Aldrich (Oakville, ON, Canada). Sodium hydroxide (>97.0%) and urea (>99.6%) were purchased from Fisher Scientific (Mississauga, ON, Canada). Distilled water was utilized throughout this study.

2.2. Preparation of wood cellulose films

The wood pulp (2 g) was placed in 200 mL of H_2SO_4 solution for 48 hours at 25 °C

with continuous stirring at 200 rpm to reduce the molecular weight of cellulose via hydrolysis, where the concentrations of H_2SO_4 solutions were 30 wt.% for aspen, pine and spruce pulps, and 25 wt.% for eucalyptus and maple pulps. After acid hydrolysis, the samples were thoroughly washed with water, dried in an oven at 100 °C for 16 hours, and dissolved (4 wt.%) in the aqueous solution containing NaOH/urea/H_2O in a 7:12:81 weight ratio. The solvent and wood pulps were pre-cooled to -20 °C and stirred at 2000 rpm for 8 minutes. The obtained solutions were centrifuged at 1000 rpm for 5 minutes (25 °C) to degas and precipitate the insoluble fractions, and then cast on the glass plate and coagulated in 5 wt.% H_2SO_4 aqueous bath at 25 °C for 5 minutes to produce RC films. In one treatment, the wet RC films prepared from aspen, eucalyptus, maple, pine, and spruce were air dried at 25 °C and coded as RC-A-AD, RC-E-AD, RC-M-AD, RC-P-AD, RC-S-AD, respectively. In another aspect, the wet films were dried between two stainless steel plates of a hot press machine (3895, Carver Inc., USA) at 90 °C and 0.4 MPa for 10 minutes, followed by hot pressing at 120 °C and 18 MPa for 10 minutes. The hot-pressed RC films were labelled as RC-A-HP, RC-E-HP, RC-M-HP, RC-P-HP, RC-S-HP, respectively.

2.3. Characterization of wood cellulose films

The recovery rate of cellulose after acid hydrolysis was calculated using a gravimetric method by the Equation (1):

$$Recovery\ rate\ (\%) = \frac{W_2}{W_1} \times 100\% \quad (1)$$

Where W_1 is the dry weight of wood pulps before acid hydrolysis, and W_2 is the dry weight of wood pulps after acid hydrolysis.

Before viscosity-average molecular weight (M_v) measurement, original wood pulps, acid hydrolyzed wood pulps, and hot-pressed RC films were stored at 25 °C and 50% RH for 4 days to ensure same water content. The intrinsic viscosity [η] of each sample was conducted according to the TAPPI T230 standard test method. The degree of polymerization (DP) was determined by the Mark-Houwink-Sakurada equation, and

the M_v values were calculated by multiplying DP by the molar mass of anhydrous glucose unit (162 g/mol).

$$DP^{0.9} = 1.65[\eta] \quad (2)$$

Before density measurement, RC films (5 cm × 5 cm) were conditioned at 25 °C and 50% RH for 4 days. The thickness of the films was determined with a micrometer (resolution of 0.001 mm, Mitutoyo 547-400S, Japan) at 10 random points. The density was calculated by the ratio of weight and volume, and the apparent porosity was calculated based on the densities of RC films (ρ_f) and crystalline cellulose (ρ_c = 1.63 g/cm^3) as shown in Equation (3) (Aulin, Gällstedt, & Lindström, 2010):

$$Porosity\ (\%) = \frac{\rho_c - \rho_f}{\rho_c} \times 100\% \quad (3)$$

The FT-IR spectra of RC films were recorded on an Agilent Technologies Cary 630 FT-IR spectrometer (Agilent Technologies Inc., CA, USA) as the average of 64 scans with a resolution of 2 cm^{-1}. The crystalline profile of wood pulps and RC films was measured using a high-resolution X-ray diffractometer (Empyrean, Malvern Panalytical Ltd, Malvern, UK) with copper Kα radiation (1.54178 Å) in 2θ ranging from 4° to 40°. The surface morphology of RC films was observed by a Hitachi TM1000 SEM (Hitachi Co. Ltd., Tokyo, Japan) with an acceleration voltage of 4 kV. The samples were sputter-coated with a 4 nm layer of gold-palladium using a Leica EM ACE200 coater (ON, Canada) prior to observation.

The tensile strength, elongation at break, and Young's modulus of RC films were tested at 25 °C and 50% RH by using an ADMET MTEST Quattro eXpert 7600 single-column testing system (MA, USA) with a load cell of 250 lb. and a crosshead speed of 5 mm/min. The water vapor permeability (WVP) of RC films was determined based on the ASTM E96-92 standard (ASTM, 1995). A dried film was taped on the top of a glass flask containing 3 g of anhydrous calcium chloride. The sealed glass flask was then located in a desiccator with water to reach a relative humidity of 100%. The weight change of the flask was recorded periodically at 25 °C. The WVP (g m^{-1} h^{-1} Pa^{-1}) of

films was calculated by the Equation (4):

$$WVP = \frac{\Delta m \times k}{A \times \Delta T \times \Delta P} \quad (4)$$

Where Δm is the weight change of the flask (g) during time ΔT (h), k is the thickness of each RC film (m), A is the exposed area of the film (7.85×10^{-5} m^2), and ΔP is the partial water vapor pressure difference between two sides of the film (Pa). The oxygen transmission rate (OTR) of RC films was determined at 23 °C and 0% RH using the Mocon Ox-Tran Model 2/22 (Mocon, Minneapolis, USA). The oxygen permeability (OP) was calculated by the Equation (5):

$$OP = \frac{OTR \times \ell}{\Delta P'} \quad (5)$$

where OTR is oxygen transmission rate, ℓ is the film thickness, and $\Delta P'$ is the partial pressure of oxygen (kPa).

2.4. Study of shelf life

The evaluation of the preservation effect of cellulose films on fruits was based on the methods of Guo et al. (2020) with slight modifications. Fresh cherry tomatoes washed with deionized water were placed in glass jars and covered with polyvinyl chloride plastic wrap (Kirkland Signature Stretch-Tite Plastic Wrap - 11 7/8 x750 Feet) and RC-P-HP. The tomatoes without any package were set as the control. All samples were stored at 25 °C and 50% RH for a maximum of 3 weeks to monitor the appearance and weight loss.

2.5. Statistical analysis

Each measurement was performed in triplicate, and the experimental data were presented as the mean ± standard deviation. Analysis of variance (ANOVA) was applied for the statistical analysis, followed by multiple comparison tests via Duncan's multiple-range test. All the analyses were carried out through SPSS statistical software (version 26, IBM SPSS Inc., New York, NY) with significant differences within samples at $p < 0.05$.

3. Results and discussion

As listed in Table 1, all the samples had a high recovery rate (~90%) after acid hydrolysis. The M_v values of original wood pulps ranged from 2.87×10^5 to 6.28×10^5 g/mol, which decreased to the range of 1.53×10^5 to 2.33×10^5 g/mol after acid hydrolysis. The molecular weight of hot-pressed RC films was relatively lower because a few insoluble fractions (~0.3%) were removed by centrifugation and the slight degradation happened during dissolution and regeneration process (Wang, Zhao & Deng, 2008).

Table 1. Recovery rate and molecular weight (M_v) of wood pulps and hot-pressed films.

Wood pulps	Recovery rates (%)	M_v (g/mol)		
		Original wood pulps	After acid hydrolysis	Hot-pressed films
Aspen	89.53 ± 0.35	6.28×10^5	2.33×10^5	1.70×10^5
Eucalyptus	92.25 ± 1.11	4.41×10^5	1.53×10^5	1.15×10^5
Maple	90.01 ± 1.73	2.87×10^5	1.70×10^5	9.23×10^4
Pine	91.85 ± 2.01	5.26×10^5	1.90×10^5	1.46×10^5
Spruce	92.42 ± 1.86	4.54×10^5	1.85×10^5	7.51×10^4

The average thickness of RC films produced by air-drying was 33 ± 3 μm, while the hot-pressed RC films were significantly thinner (27 ± 1 μm). As shown in Fig. 1, different sources of wood pulps did not affect the density and porosity of RC films, but the hot pressing treatment remarkably increased the density from approximately 0.95 g/cm^3 to 1.15 g/cm^3 and reduced the porosity from about 35% to 22.5%. Similar results have been reported that RC films dried with applied pressure could form dense structures (Shahi, Min, Sapkota, & Rangari, 2020). The decreased free space and cavities in RC films could contribute to the improvement in mechanical strength and gas barrier properties (Aulin et al., 2010; Wakabayashi, Fujisawa, Saito, & Isogai, 2020).

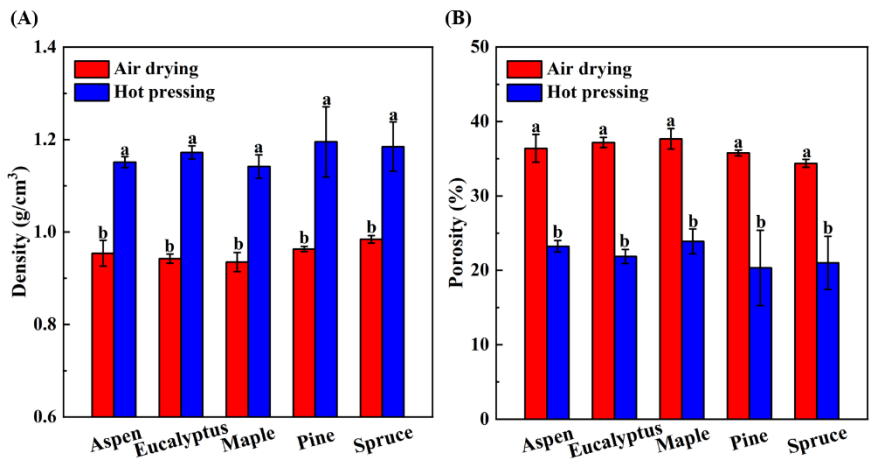

Fig. 1. Density (A) and porosity (B) of RC films. Different letters on the tops of columns represented the significant difference ($p < 0.05$).

FT-IR spectra and XRD diffraction patterns of various wood pulps and RC films were collected to investigate the effects of cellulose dissolution and regeneration in NaOH/urea aqueous solution and different drying methods on cellulose structure. As shown in Fig. 2 A-C, all samples displayed similar FT-IR spectra with no new peaks after dissolution, regeneration and drying, which demonstrated no chemical modifications happened during film production. However, changes in the intensity of the peaks were observed. For instance, the intensities of absorption peaks at around 3360 and 3269 cm^{-1} decreased after dissolution and regeneration, while the hot-pressed films presented even lower intensities than the air-dried films. These two peaks were attributed to the O-H stretching vibration of the hydroxyl groups, which indicated the intra- and intermolecular hydrogen bonds in cellulose, respectively (Zhou & Wang, 2021). The hydrogen bonds were broken during the dissolution, and the rearrangement happened during the regeneration and drying process. The rapid coagulation and drying process of RC films led to the disturbed intermolecular interaction and decreased intensities at 3330 and 3269 cm^{-1} (Lindman, Medronho, Alves, Costa, Edlund, & Norgren, 2017). Besides, the peak at 1427 cm^{-1} was the absorption band of the crystalline cellulose due to asymmetric -CH_2 bending vibration, while the peak at 898 cm^{-1} was the -C-O-C- bridge stretching, representing the amorphous region and

cellulose II crystalline structure (Salim, Asik, & Sarjadi, 2021) The ratio of peak intensities at 1427 and 898 cm^{-1} was defined as "crystallinity index", which was decreased after dissolution and regeneration, indicating the decrease in crystallinity and the transition from cellulose I to cellulose II structure (Salim et al., 2021; Zhou et al., 2021). As shown in Fig. 2 D-E, the wood pulps displayed similar diffraction peaks at about 14.8° ($1\bar{1}0$), 16.3° (110), 22.5° (200), and 34° (040), which were typical cellulose I structure (Zhou et al., 2021). After the dissolution and regeneration process, the RC films showed cellulose II structure with broad diffraction peaks at 20.2° and 22.6°, corresponding to (110) and (020) crystallographic planes, respectively (Razali et al., 2022). The crystallinity indices (CI) of RC films were significantly lower than those of the wood pulps. It indicated a crystal transformation of cellulose I to cellulose II during dissolution and regeneration, which was in accordance with the FT-IR results. The sources of wood pulps did not affect the diffraction patterns of RC films.

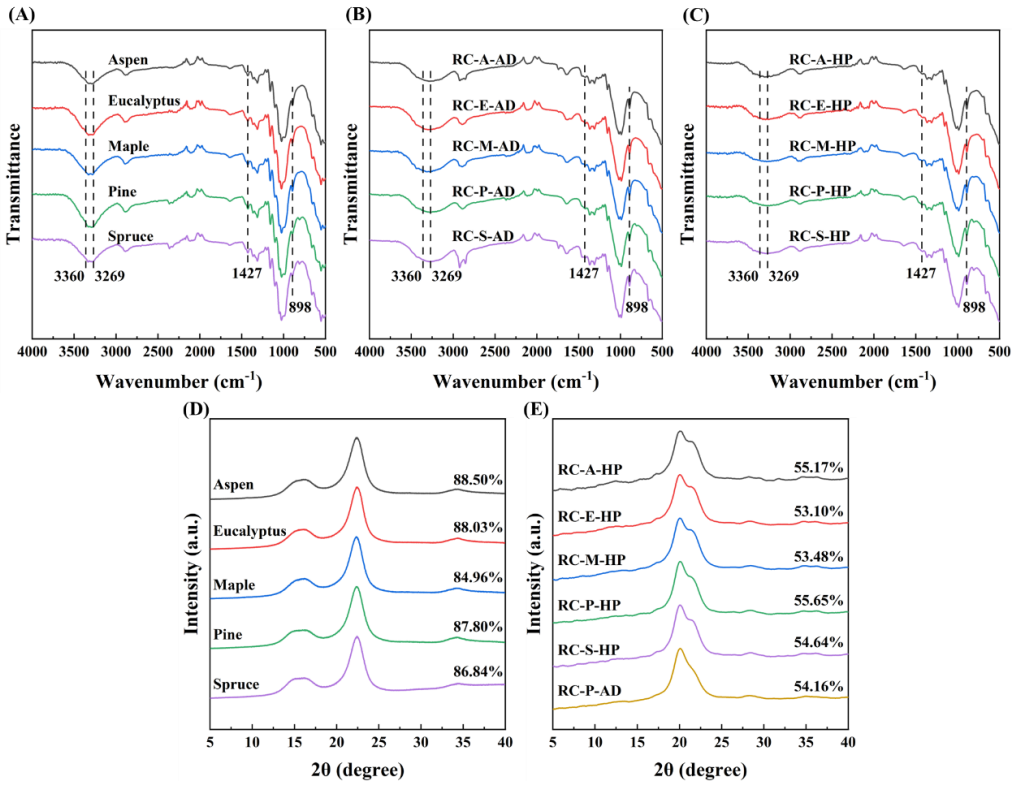

Fig. 2. Fourier transform infrared spectroscopy spectra of wood pulp cellulose (A), air-dried RC films (B), and hot-pressed RC films (C). X-ray diffraction patterns and

crystallinity index of wood cellulose pulps (D) and RC films (E).

The morphology of RC films dried by different methods was observed by SEM. As shown in Fig. 3 A, no obvious undissolved fibers were observed on the surface of RC films, indicating a good solubility of hydrolyzed wood pulp cellulose in NaOH/urea aqueous solution. However, the air-dried RC films showed uneven and rough surfaces and layered cross-sections (Fig. 3 B), which might be due to the inevitable non-uniform shrinkage during the air-drying process (Ketola et al., 2018). In contrast, the hot-pressed RC films possessed smooth and uniform surfaces and dense internal structures. It was because the hot pressing treatment could facilitate the stretch and rearrangement of cellulose chains and effectively reduce the free space and cavities in the RC films (Wang et al., 2013). Moreover, the air-dried RC films were not as transparent as the hot-pressed ones (Fig. 3 C). It was due to the uneven structure and larger thickness of air-dried RC films. The high transparency of RC films is beneficial for displaying the food products in packaging.

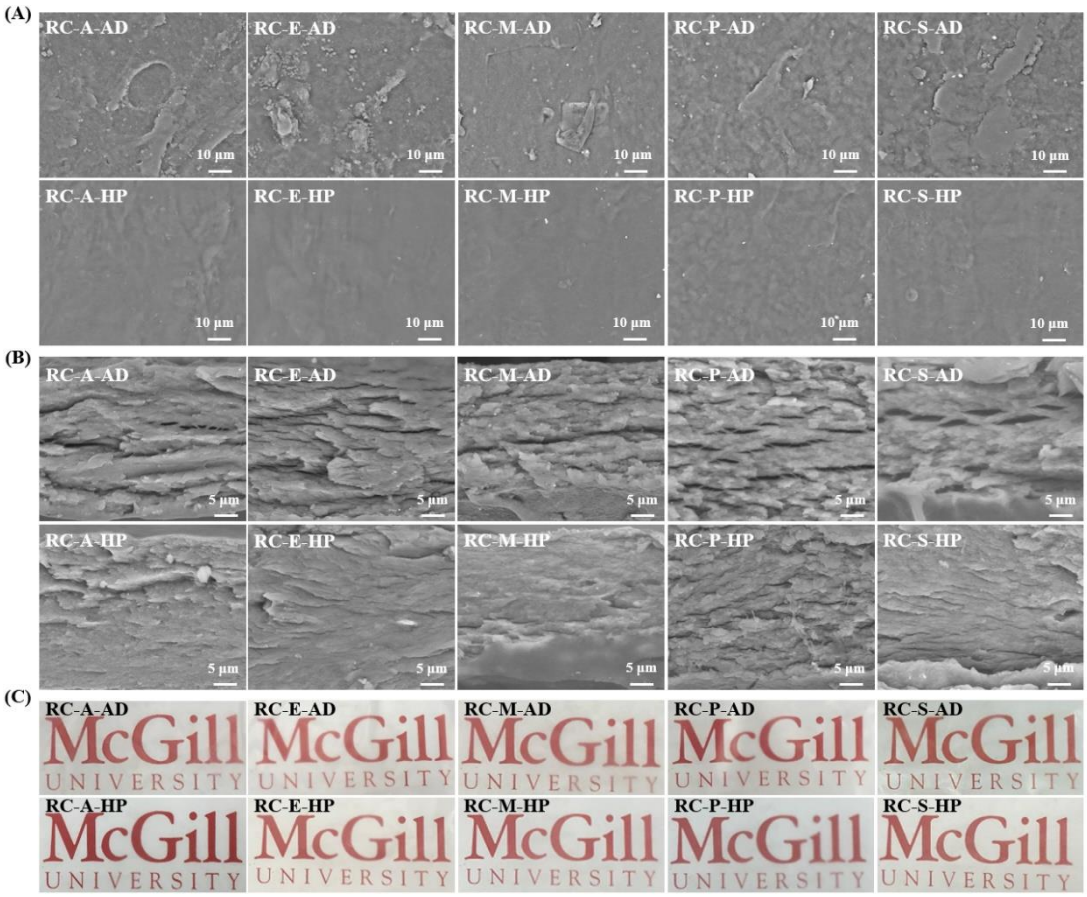

Fig. 3. SEM images of RC films: surface (A) and cross-section (B). Photos of RC films (C).

The mechanical properties of RC films are essential because food packaging materials need to maintain the integrity and preserve the quality of packaged food (Ai et al., 2021). As shown in Fig. 4 A and Fig. 4 C, the tensile strength and Young's modulus of RC films produced from pine were significantly higher than those of other RC films. It might be due to the variation of molecular weight and CI of cellulose from different sources (Aulin et al., 2010; De Silva & Byrne, 2017; Mokhena, Sadiku, Mochane, Ray, John, & Mtibe, 2021; Yousefi, Faezipour, Hedjazi, Mousavi, Azusa, & Heidari, 2013). For example, the higher M_v value of cellulose could enhance the intermolecular entanglement, leading to an improved tensile strength of cellulose film (Jin et al., 2019); however, the aggregation and entanglement of cellulose chains also restricted the molecular orientation during dissolution and regeneration processes, and resulted in the decreased tensile strength (Xie et al. 2021). At the same time, the high content of the

crystalline structure led to an enhanced tensile strength (Shi et al., 2021). As expected, the hot-pressed RC films possessed notable enhancement in tensile strength and modulus compared to the air-dried films. These different mechanical properties were attributed to the density and porosity (Cazón, Velazquez, & Vázquez, 2019). It has been demonstrated that pores and free volume affects the mechanical properties of the material, since the less solid material per unit volume, the weaker the resistance to deformation (Cao et al., 2020; Su, Rao, He, & Wei, 2020). The RC-P-HP sample exhibited the highest tensile strength of 85.00 ± 3.26 MPa and Young's modulus of 6.45 ± 0.36 GPa and was stronger than the RC films fabricated from bamboos in DMAc/LiCl solvent (81.09 MPa) (Gao, Li, Zhang, Tang, & Chen, 2021), corncob residue in ionic liquid (70.63 MPa) (Song, Chen, Chen, Xu, & Xu, 2021), bed sheets in NaOH/urea solution (76.21 MPa) (Zhou et al., 2021), and cotton linter pulps in NaOH/urea solution (73.40 MPa) (Reddy, Varada Rajulu, Rhim, & Seo, 2018).

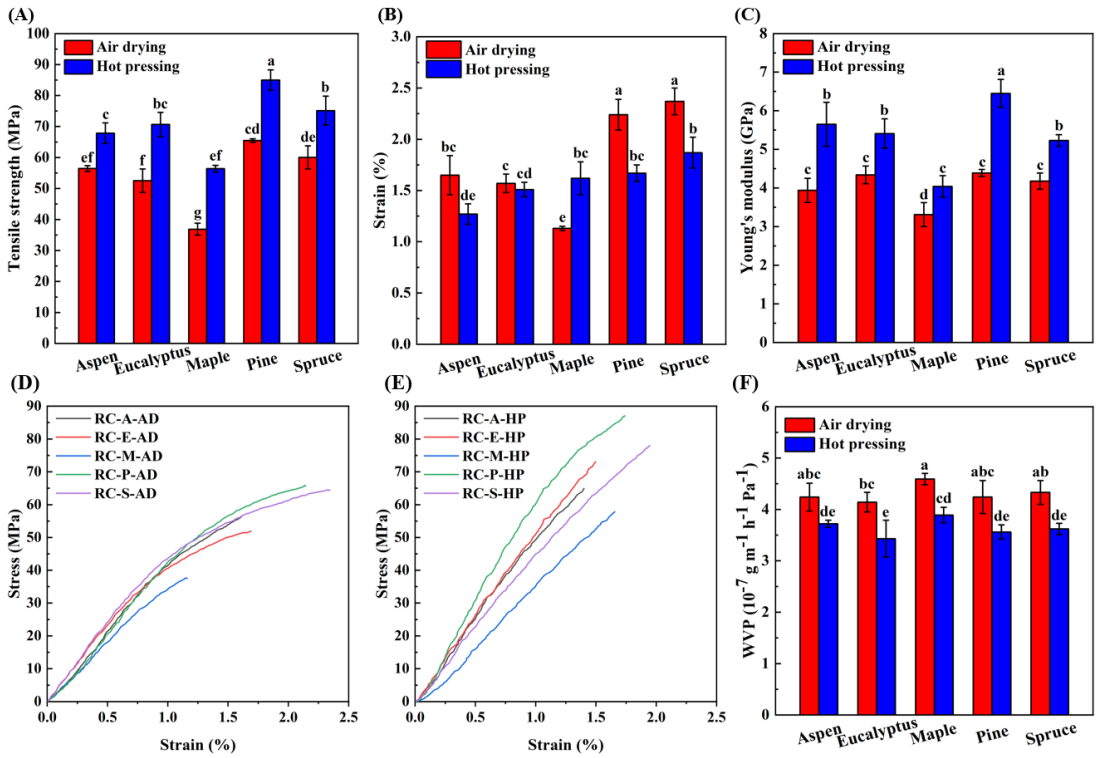

Fig. 4. Mechanical properties (A-E) and WVP (F) of RC films. Different letters on the tops of columns represented the significant difference ($p < 0.05$).

The WVP values of RC films dried by different methods are shown in Fig. 4 F. Despite the sources of wood pulps, the air-dried RC films displayed similar WVP values ranging from 4.14 ± 0.19 to 4.59 ± 0.11 × 10^{-7} g m^{-1} h^{-1} Pa^{-1}, while the hot pressing treatment significantly decreased the values to the range of 3.43 ± 0.36 to 3.89 ± 0.15 × 10^{-7} g m^{-1} h^{-1} Pa^{-1}. The hot-pressed films had reduced apparent porosity, which slowed down the diffusion of water vapor. It is well known that the water vapor barrier property of cellulose films is not ideal because of their hydrophilic nature, and chemical modifications are usually required (Li, Wang, Wang, Qin, & Wu, 2019). The improvement in barrier properties through hot pressing treatment could avoid using chemical reagents and eliminate possible contamination from chemical residues. It was worth noting that the WVP values of most RC films in this work were lower than those of RC films manufactured from oil palm biomass (4.68 × 10^{-7} g m^{-1} h^{-1} Pa^{-1}) (Amalini, Haida, Imran, & Haafiz, 2019) and cotton linter pulp (8.21 × 10^{-6} g m^{-1} h^{-1} Pa^{-1}) (Reddy et al., 2018).

Packaging materials with suitable mechanical and barrier properties can protect food products from physical damage, oxidation, loss of nutrients, and dehydration, and thereby extend the shelf life (Pandey, Sharma, & Gundabala, 2022; Yilmaz, Demirhan, & Ozbek, 2022). Based on the above-mentioned results, the RC-P-HP film with relatively good tensile strength and water vapor barrier property was selected for the shelf-life study and comparison with commercial plastic wrap. As shown in Fig. 5 A, the unpackaged cherry tomatoes became soft and exhibited obvious wrinkles on the surface on day 10, and completely deteriorated with a putrid odor on day 16. However, the tomatoes packaged with plastic wrap and RC-P-HP film well maintained their bright red color and hardness on day 10, and only showed minor shrinkages without putridity on day 16. The dehydration of fruits affects their shelf life and commercial value (Fich, Fisher, Zamir, & Rose, 2020). The weight loss of unwrapped and packaged cherry tomatoes over 16 days was monitored and displayed in Fig. 5 B. The unwrapped tomatoes lost about 21.72% of their original weight on day 16. This was lowered to

10.40% and 11.25% when commercial plastic wrap and RC-P-HP film were applied, respectively. The weight loss of cherry tomatoes was mainly due to water loss from transpiration and respiration processes. The WVP value of RC-P-HP ($3.56 \pm 0.14 \times 10^{-7}$ g m^{-1} h^{-1} Pa^{-1}) was higher than the plastic wrap ($2.37 \pm 0.17 \times 10^{-8}$ g m^{-1} h^{-1} Pa^{-1}). However, the OTR value of plastic wrap exceeded the detection limit (2000 cc/m^2 day), and its OP value was higher than 0.02 cc m^{-1} day^{-1} atm^{-1} compared to $3.01 \pm 0.49 \times 10^{-5}$ cc m^{-1} day^{-1} atm^{-1} for RC-P-HP. It was reported that the composite film of gelatin and carboxymethyl cellulose with a WVP value of 5.47×10^{-7} g m^{-1} h^{-1} Pa^{-1} and OP of 1.32×10^{-4} cc m^{-1} day^{-1} atm^{-1} led to 23.22% weight loss of packed cherry tomatoes after 14 days' storage (Samsi et al., 2019). Thus, RC-P-HP effectively prevented the weight loss of cherry tomatoes due to the significantly reduced OP and relatively low WVP values.

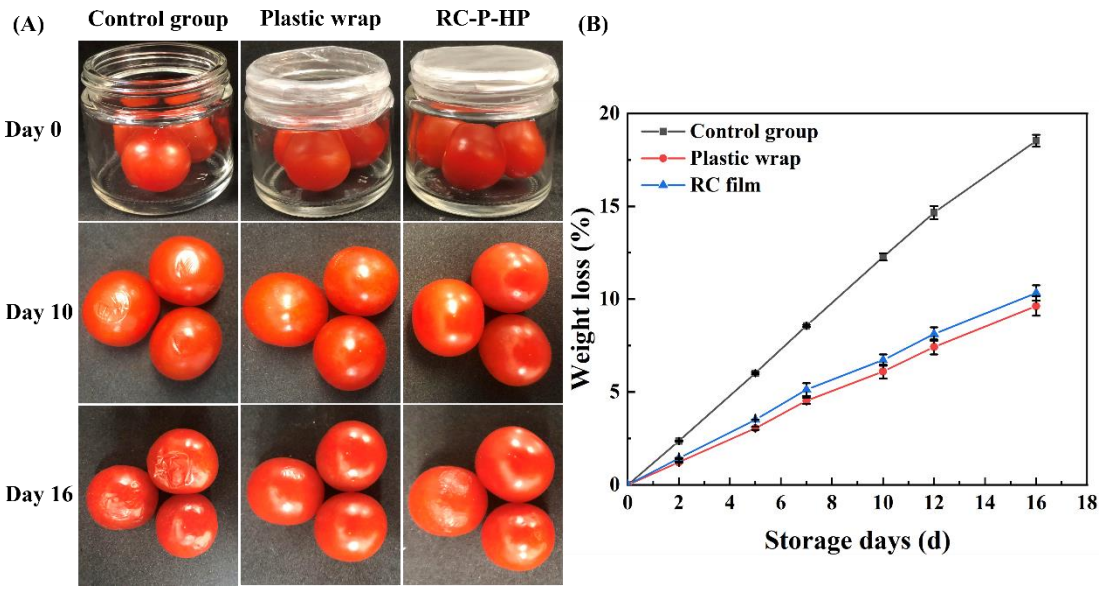

Fig. 5. Appearance (A) and weight loss (B) of cherry tomatoes under different packaging conditions.

4. Conclusion

After acid hydrolysis, five wood pulps were successfully dissolved in NaOH/urea aqueous solution. The type of wood pulps showed no remarkable impact on the structure of RC films, and all films were transparent for displaying the packaged products. Furthermore, the hot pressing process resulted in the RC films with smoother

surfaces and fewer cavities compared to the air-dried films, which contributed to the dramatically improved mechanical strength and water vapor barrier property. Among all the samples, the RC-P-HP film made from pine showed the best properties and could effectively prevent the weight loss and deterioration of the wrapped cherry tomatoes for up to 16 days. This performance was comparable to the commercial plastic wrap, and thus the hot-pressed RC films had the potential applications in biodegradable food packaging.

Conflict of Interest

The authors declare that they have no conflict of interest.

Acknowledgement

We would like to acknowledge financial support from the Fonds de Recherche du Quebec - Nature et Technologies (2021-PR-283095), Canada Foundation for Innovation (39173), and Mitacs Accelerate (FR68649). We would like to acknowledge McGill University ECP3 Multi-Scale Imaging Facility for the image acquisition.

References

Ai, B., Zheng, L., Li, W., Zheng, X., Yang, Y., Xiao, D., Shi, J., & Sheng, Z. (2021). Biodegradable cellulose film prepared from banana pseudo-stem using an ionic liquid for mango preservation. *Frontiers in Plant Science, 12*, 234. DOI: 10.3389/fpls.2021.625878

Amalini, A.N., Haida, M.K.N., Imran, K., & Haafiz, M.K.M. (2019). Relationship between dissolution temperature and properties of oil palm biomass based-regenerated cellulose films prepared via ionic liquid. *Materials Chemistry and Physics, 221*, 382-389. DOI: 10.1016/j.matchemphys.2018.09.028

ASTM. (1995). Standard test methods for water vapor transmission of material, E96-95. *Annual book of ASTM standards, 4*, 697-704.

Aulin, C., Gällstedt, M., & Lindström, T. (2010). Oxygen and oil barrier properties of microfibrillated cellulose films and coatings. *Cellulose, 17*(3), 559-574. DOI: 10.1007/s10570-009-9393-y

Cai, J., & Zhang, L. (2005). Rapid dissolution of cellulose in LiOH/urea and NaOH/urea aqueous solutions. *Macromolecular Bioscience, 5*(6), 539-548. DOI: 10.1002/mabi.200400222

Cao, H., Luo, Z., Wang, C., Wang, J., Hu, T., Xiao, L., & Che, J. (2020). The stress concentration mechanism of pores affecting the tensile properties in vacuum die casting metals. *Materials, 13*(13), 3019. DOI: 10.3390/ma13133019

Cazón, P., Velazquez, G., & Vázquez, M. (2019). Novel composite films from regenerated cellulose-glycerol-polyvinyl alcohol: Mechanical and barrier properties. *Food Hydrocolloids, 89*, 481-491. DOI: 10.1016/j.foodhyd.2018.11.012

De Silva, R., & Byrne, N. (2017). Utilization of cotton waste for regenerated cellulose fibres: Influence of degree of polymerization on mechanical properties. *Carbohydrate Polymers, 174*, 89-94. DOI: 10.1016/j.carbpol.2017.06.042

Diggle, A., & Walker, T.R. (2020). Implementation of harmonized extended producer

responsibility strategies to incentivize recovery of single-use plastic packaging waste in Canada. *Waste Management, 110*, 20-23. DOI: 10.1016/j.wasman.2020.05.013

Fich, E.A., Fisher, J., Zamir, D., & Rose, J.K. (2020). Transpiration from tomato fruit occurs primarily via trichome-associated transcuticular polar pores. *Plant Physiology, 184*(4), 1840-1852. DOI: 10.1104/pp.20.01105

Gao, X., Li, M., Zhang, H., Tang, X., & Chen, K. (2021). Fabrication of regenerated cellulose films by DMAc dissolution using parenchyma cells via low-temperature pulping from Yunnan-endemic bamboos. *Industrial Crops and Products, 160*, 113116. DOI: 10.1016/j.indcrop.2020.113116

Gong, X., Wang, Y., Tian, Z., Zheng, X., & Chen, L. (2014). Controlled production of spruce cellulose gels using an environmentally "green" system. *Cellulose, 21*(3), 1667-1678. DOI: 10.1007/s10570-014-0200-z

Guo, X., Chen, B., Wu, X., Li, J., & Sun, Q. (2020). Utilization of cinnamaldehyde and zinc oxide nanoparticles in a carboxymethylcellulose-based composite coating to improve the postharvest quality of cherry tomatoes. *International Journal of Biological Macromolecules, 160*, 175-182. DOI: 10.1016/j.ijbiomac.2020.05.201

Hasan, I., Wang, J., & Tajvidi, M. (2021). Tuning physical, mechanical and barrier properties of cellulose nanofibril films through film drying techniques coupled with thermal compression. *Cellulose, 28*(18), 11345-11366. DOI: 10.1007/s10570-021-04269-9

Huang, K., & Wang, Y. (2022). Recent applications of regenerated cellulose films and hydrogels in food packaging. *Current Opinion in Food Science, 43*, 7-17. DOI: 10.1016/j.cofs.2021.09.003

Huang, W., Wang, Y., Zhang, L., & Chen, L. (2016). Rapid dissolution of spruce cellulose in H_2SO_4 aqueous solution at low temperature. *Cellulose, 23*(6), 3463-3473. DOI: 10.1007/s10570-016-1047-2

Jia, C., Chen, C., Kuang, Y., Fu, K., Wang, Y., Yao, Y., Kronthal, S., Hitz, E., Song, J., Xu, F., Liu, B., & Xu, F. (2018). From wood to textiles: Top-down assembly of aligned cellulose nanofibers. *Advanced Materials, 30*(30), 1801347. DOI: 10.1002/adma.201801347

Jin, L., Gan, J., Hu, G., Cai, L., Li, Z., Zhang, L., Zheng, Q., & Xie, H. (2019). Preparation of cellulose films from sustainable CO_2/DBU/DMSO system. *Polymers*, *11*(6), 994. DOI: 10.3390/polym11060994

Ketola, A.E., Strand, A., Sundberg, A., Kouko, J., Oksanen, A., Salminen, K., Fu, S., & Retulainen, E. (2018). Effect of micro-and nanofibrillated cellulose on the drying shrinkage, extensibility, and strength of fibre networks. *BioResources, 13*(3), 5319-5342. DOI: 10.15376/biores.13.3.5319-5342

Li, W., Wang, S., Wang, W., Qin, C., & Wu, M. (2019). Facile preparation of reactive hydrophobic cellulose nanofibril film for reducing water vapor permeability (WVP) in packaging applications. *Cellulose, 26*(5), 3271-3284. DOI: 10.1007/s10570-019-02270-x

Lindman, B., Medronho, B., Alves, L., Costa, C., Edlund, H., & Norgren, M. (2017). The relevance of structural features of cellulose and its interactions to dissolution, regeneration, gelation and plasticization phenomena. *Physical Chemistry Chemical Physics, 19*(35), 23704-23718. DOI: 10.1039/C7CP02409F

Md Salim, R., Asik, J., & Sarjadi, M.S. (2021). Chemical functional groups of extractives, cellulose and lignin extracted from native *Leucaena leucocephala* bark. *Wood Science and Technology, 55*(2), 295-313. DOI: 10.1007/s00226-020-01258-2

Missio, A.L., Mattos, B.D., Otoni, C.G., Gentil, M., Coldebella, R., Khakalo, A., Gatto, D.A., & Rojas, O.J. (2020). Cogrinding wood fibers and tannins: Surfactant effects on the interactions and properties of functional films for sustainable packaging materials. *Biomacromolecules, 21*(5), 1865-1874. DOI: 10.1021/acs.biomac.9b01733

Mokhena, T.C., Sadiku, E.R., Mochane, M.J., Ray, S.S., John, M.J., & Mtibe, A.

(2021). Mechanical properties of cellulose nanofibril papers and their bionanocomposites: A review. *Carbohydrate Polymers, 273*, 118507. DOI: 10.1016/j.carbpol.2021.118507

Muthoka, R.M., Panicker, P.S., Agumba, D.O., Pham, H.D., & Kim, J. (2021). All-biobased transparent-wood: A new approach and its environmental-friendly packaging application. *Carbohydrate Polymers, 264*, 118012. DOI: 10.1016/j.carbpol.2021.118012

Pandey, S., Sharma, K., & Gundabala, V. (2022). Antimicrobial bio-inspired active packaging materials for shelf life and safety development: A review. *Food Bioscience*, *48*, 101730. DOI: 10.1016/j.fbio.2022.101730

Qing, Y., Sabo, R., Wu, Y., Zhu, J., & Cai, Z. (2015). Self-assembled optically transparent cellulose nanofibril films: Effect of nanofibril morphology and drying procedure. *Cellulose, 22*(2), 1091-1102. DOI: 10.1016/j.carbpol.2021.118012

Razali, N.A.M., Sohaimi, R.M., Othman, R.N.I.R., Abdullah, N., Demon, S.Z.N., Jasmani, L., Yunus, W.M.Z.W., Ya'acob, W.M.H.W., Salleh, E.M., Norizan, M.N., & Halim, N.A. (2022). Comparative study on extraction of cellulose fiber from rice straw waste from chemo-mechanical and pulping method. *Polymers, 14*(3), 387. DOI: 10.3390/polym14030387

Reddy, J.P., Varada Rajulu, A., Rhim, J.-W., & Seo, J. (2018). Mechanical, thermal, and water vapor barrier properties of regenerated cellulose/nano-SiO_2 composite films. *Cellulose, 25*(12), 7153-7165. DOI: 10.1007/s10570-018-2059-x

Rol, F., Billot, M., Bolloli, M., Beneventi, D., & Bras, J. (2020). Production of 100% cellulose nanofibril objects using the molded cellulose process: A feasibility study. *Industrial & Engineering Chemistry Research, 59*(16), 7670-7679. DOI: 10.1021/acs.iecr.9b06127

Samsi, M.S., Kamari, A., Din, S.M., & Lazar, G. (2019). Synthesis, characterization and application of gelatin–carboxymethyl cellulose blend films for preservation of cherry tomatoes and grapes. *Journal of food science and technology*, *56*(6),

3099-3108. DOI: 10.1007/s13197-019-03809-3

Shahi, N., Min, B., Sapkota, B., & Rangari, V.K. (2020). Eco-friendly cellulose nanofiber extraction from sugarcane bagasse and film fabrication. *Sustainability, 12*(15), 6015. DOI: 10.3390/su12156015

Shi, Z., Liu, Y., Xu, H., Yang, Q., Xiong, C., Kuga, S., & Matsumoto, Y. (2018). Facile dissolution of wood pulp in aqueous NaOH/urea solution by ball milling pretreatment. *Industrial Crops and Products, 118*, 48-52. DOI: 10.1016/j.indcrop.2018.03.035

Shi, S.C., Chen, C., Zhu, J.L., Li, Y., Meng, X., Huang, H.D., & Li, Z.M. (2021). Environmentally friendly regenerated cellulose films with improved dielectric properties via manipulating the hydrogen bonding network. *Applied Physics Letters, 119*(2), 022903. DOI: 10.1063/5.0056164

Shi, H., Wu, L., Luo, Y., Yu, F., & Li, H. (2022). A facile method to prepare cellulose fiber-based food packaging papers with improved mechanical strength, enhanced barrier, and antibacterial properties. *Food Bioscience*, *48*, 101729. DOI: 10.1016/j.fbio.2022.101729

Song, Y., Chen, S., Chen, Y., Xu, Y., & Xu, F. (2021). Biodegradable and transparent films with tunable UV-blocking property from Lignocellulosic waste by a top-down approach. *Cellulose, 28*(13), 8629-8640. DOI: 10.1007/s10570-021-03994-5

Su, S.-l., Rao, Q.-h., He, Y.-H., & Wei, X. (2020). Effects of porosity on tensile mechanical properties of porous FeAl intermetallics. *Transactions of Nonferrous Metals Society of China, 30*(10), 2757-2763. DOI: 10.1016/S1003-6326(20)65418-8

Tang, X., Liu, G., Zhang, H., Gao, X., Li, M., & Zhang, S. (2021). Facile preparation of all-cellulose composites from softwood, hardwood, and agricultural straw cellulose by a simple route of partial dissolution. *Carbohydrate Polymers, 256*, 117591. DOI: 10.1016/j.carbpol.2020.117591

Tayeb, A.H., Tajvidi, M., & Bousfield, D. (2020). Paper-based oil barrier packaging using lignin-containing cellulose nanofibrils. *Molecules, 25*(6), 1344. DOI: 10.3390/molecules25061344

Wakabayashi, M., Fujisawa, S., Saito, T., & Isogai, A. (2020). Nanocellulose film properties tunable by controlling degree of fibrillation of TEMPO-oxidized cellulose. *Frontiers in Chemistry, 8*, 37. DOI: 10.3389/fchem.2020.00037

Wang, Q., Cai, J., Zhang, L., Xu, M., Cheng, H., Han, C.C., Kuga, S., Xiao, J., & Xiao, R. (2013). A bioplastic with high strength constructed from a cellulose hydrogel by changing the aggregated structure. *Journal of Materials Chemistry A, 1*(22), 6678-6686. DOI: 10.1039/C3TA11130J

Wang, Y., Zhao, Y., & Deng, Y. (2008). Effect of enzymatic treatment on cotton fiber dissolution in NaOH/urea solution at cold temperature. *Carbohydrate Polymers, 72*(1), 178-184. DOI: 10.1016/j.carbpol.2007.08.003

Xie, K., Tu, H., Dou, Z., Liu, D., Wu, K., Liu, Y., Chen, F., Zhang, L., & Fu, Q. (2021). The effect of cellulose molecular weight on internal structure and properties of regenerated cellulose fibers as spun from the alkali/urea aqueous system. *Polymer*, *215*, 123379. DOI: 10.1016/j.polymer.2021.123379

Yilmaz, P., Demirhan, E., & Ozbek, B. (2022). Development of *Ficus carica* Linn leaves extract incorporated chitosan films for active food packaging materials and investigation of their properties. *Food Bioscience*, *46*, 101542. DOI: 10.1016/j.fbio.2021.101542

Yousefi, H., Faezipour, M., Hedjazi, S., Mousavi, M.M., Azusa, Y., & Heidari, A.H. (2013). Comparative study of paper and nanopaper properties prepared from bacterial cellulose nanofibers and fibers/ground cellulose nanofibers of canola straw. *Industrial Crops and Products, 43*, 732-737. DOI: 10.1016/j.indcrop.2012.08.030

Zhou, C., & Wang, Y. (2021). Recycling of waste cotton fabrics into regenerated cellulose films through three solvent systems: A comparison study. *Journal of*

497 *Applied Polymer Science, 138*(48), 51255. DOI: 10.1002/app.51255